LANGMUIR

pubs.acs.org/Langmuir Article

Self-Assembly and Crystallization of DNA-Coated Colloids via Linker-Encoded Interactions

Janna Lowensohn, Alexander Hensley, Michael Perlow-Zelman, and W. Benjamin Rogers*

Cite This: https://dx.doi.org/10.1021/acs.langmuir.9b03391 Read Online

ACCESS | Metrics & More | Article Recommendations | Supporting Information

Downloaded via BRANDEIS UNIV on February 18, 2020 at 20:40:27 (UTC).
See https://pubs.acs.org/sharingguidelines for options on how to legitimately share published articles.

ABSTRACT: Coating colloidal particles with DNA is a promising strategy to make functional nanoscale materials because the particles can be programmed to spontaneously self-assemble into complex, ordered structures. In this Article, we explore the phase behavior and types of structures that can be formed when interactions between DNA-coated colloids are specified by linker DNA strands dispersed in solution. We show that linker-mediated interactions direct the self-assembly of colloids into equilibrium crystal structures. Furthermore, we demonstrate how different linker sequences and concentrations produce different crystal lattices, whose symmetry and compositional order are encoded exclusively by the linker-mediated interactions. These results illustrate how linkers can be used to separate the assembly instructions, encoded in the linkers, from the colloids themselves. We also examine the phase behavior of asymmetric linkers, which bind more strongly to one colloidal species than the other. We find that asymmetry strongly influences the concentration dependence of the colloidal interactions, which we explain using a mean-field model. We also find evidence that asymmetric linkers might help to reduce kinetic bottlenecks to colloidal crystallization. Together, our findings expand the design rules of linker-mediated self-assembly and make connections between the various schemes for programming assembly of DNA-coated colloids reported in the literature.

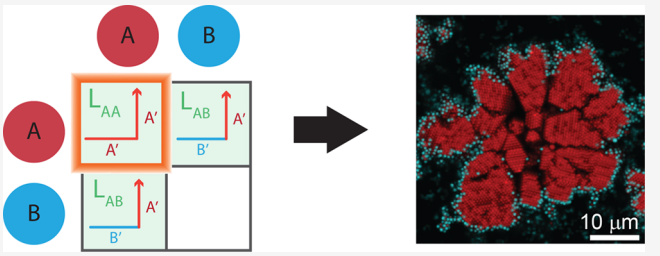

INTRODUCTION

DNA is a powerful tool for assembling user-specified mesoscale structures.[1,2] Owing to base pairing, adenine with thymine and cytosine with guanine, single-stranded DNA molecules bind specifically to their complementary sequences.[3] Coating microscopic colloidal particles with complementary sequences of single-stranded DNA can therefore induce specific, attractive interactions between the particles.[4,5] These interactions drive the particles to self-assemble into ordered, often periodic, mesoscale structures. This approach has been used to construct a variety of colloidal crystals with specified symmetries, lattice parameters, and compositions.[6−12] In principle, user-prescribed, aperiodic structures could also be assembled from complex mixtures of colloids through the rational design of their interactions,[13−15] but these structures have not been made in practice.

The creation of more complex prescribed structures from DNA-coated colloids requires one to overcome significant hurdles. Theoretical work has shown that to produce aperiodic structures with high yield from uniformly coated particles, each particle in the target structure must have specific, attractive interactions that bind the particle only to its neighbors in the final design.[13,14] The interactions must be chosen to prevent binding between non-neighboring particles. However, it is intractable to encode the requisite set of interactions in the DNA sequences grafted to the colloids' surfaces. There are two main obstacles to using direct binding of grafted sequences: (1) It is challenging to match all of the mutual interactions, owing to intrinsic sequence-to-sequence differences in the DNA binding affinities[3] and inevitable batch-to-batch variations in the DNA grafting densities.[16,17] (2) There are a limited number of interactions that can be encoded using DNA, owing to the limited number of orthogonal DNA sequences.[18] In order to overcome these hurdles, new approaches are required.

An alternative strategy is to coat particles with grafted sequences that are not complementary and induce binding between particles using linkers, DNA strands dispersed in solution. In this design paradigm, each particle species is uniformly coated with a single sequence of DNA, which uniquely identifies each particle species but does not encode any pair interactions. Instead, all pair interactions are encoded in linker sequences that bind the grafted strands together. Each linker is designed with two binding domains, which are complementary to particle-identification sequences.[6,19−21] When these two domains bind with their complementary grafted strands, the two associated particles are bound by the resulting DNA bridge. The linker binding domains can be

Special Issue: Advances in Active Materials

Received: October 31, 2019
Revised: February 4, 2020
Published: February 4, 2020

© XXXX American Chemical Society

symmetric, forming an equal number of base pairs within each domain,[1,2,6,19] or asymmetric, forming an unequal number of base pairs within each domain.[7,18,22−27]

A recent article from our group showed that linker-mediated binding can help to overcome the obstacles mentioned above.[21] Specifically, we showed that the strength of linker-mediated interactions can be tuned by dozens of k_BT by changing the linker sequences and concentrations, providing a strategy for overcoming the variability in the DNA affinity and coating density. We also showed that linker sequences can prescribe orthogonal interactions within a complex mixture of various linker types, suggesting that linker-mediated assembly should require fewer unique DNA sequences than direct binding to specify the same number of specific interactions. Taken together, these results support the claim that linkers are a powerful tool for programming and matching the myriad interactions required to assemble user-prescribed structures. However, because we used only symmetric linkers and inferred their interactions from measurements of the melting temperature between a colloidal gel and a colloidal gas, some important questions remain: Do linker-mediated interactions direct self-assembly of equilibrium structures, like crystals, or do they get trapped in gel states? Can different linker combinations produce different crystal phases from the same set of colloidal particles? Also, what are the essential differences between symmetric and asymmetric linkers?

In this Article, we show that linkers can indeed direct the self-assembly of many crystal phases and we characterize the similarities and differences between symmetric and asymmetric linkers. Specifically, we show that symmetric linkers direct the assembly of binary colloidal crystals over a range of linker concentrations. We find that DNA-coated colloids fail to crystallize at the lowest linker concentrations, which we hypothesize is due to kinetic limitations in the dissociation of DNA bridges. We show that the crystal structures can be tuned by changing the linker species and their concentrations in solution. Finally, we explore what happens when we make one side of the linker bind more strongly than the other by adjusting the length of the linker binding domains. Here, we find that the phase behavior becomes less dependent on the linker concentration as the asymmetry increases. A previous model[21] shows that this change in behavior corresponds to a transition in which linkers preferentially coat one particle species instead of remaining free in solution. The net result is a phase behavior that approaches that of the direct-binding case, which could limit the utility of asymmetric linkers for fully addressable assembly. However, we also find evidence that asymmetric linkers may help to overcome kinetic barriers and direct assembly of crystals even at low linker concentrations.

EXPERIMENTAL SECTION

Our experimental system consists of two sequences of single-stranded DNA, referred to as A and B, which are grafted to colloidal particles, and single-stranded DNA "linker" sequences dispersed in solution (Figure 1A). Each grafted sequence is 65 bases long and consists of a 54 thymine spacer followed by a unique 11 nucleotide (nt) "sticky end". The linker sequences are composed of two binding domains, one complementary to A and the other complementary to B. Each binding domain can vary from 7 to 15 nt in length, and the two binding domains are separated from one another by a single unpaired nucleotide for flexibility. See Table S1 for all DNA sequences.

The linker-mediated interactions that emerge between DNA-coated colloids are temperature dependent. The particles assemble at low temperatures and disassemble at high temperatures. We define the melting temperature (T_m) as the temperature at which 50% of the particles are unbound.[16] Because the full transition from solid to gas is narrow, less than 1 °C wide, we identify the melting temperature as the lowest temperature at which at least 50% of the colloids are unbound, giving an uncertainty in T_m of at most 1 °C (Figure 1B). We characterize this temperature-dependent phase behavior, as well as the structures that form, using a combination of brightfield and confocal fluorescence microscopy.

We perform experiments at a total particle concentration of 0.5% by volume and suspend the particles in Tris-EDTA buffer containing 500 mM NaCl. For all crystallization experiments, we use 600 nm-diameter polystyrene colloids grafted with DNA using the method from Pine and co-workers[28] since the DNA coupling efficiency is high and the smaller particles assemble rapidly. For all melting-temperature measurements with asymmetric linkers, we use 1 μm-diameter polystyrene colloids prepared using the method from Crocker and co-workers.[29] We choose this method so that we can compare our present results to previous reports.[21] See the Supporting Information for descriptions of our synthesis protocols and experimental methods.

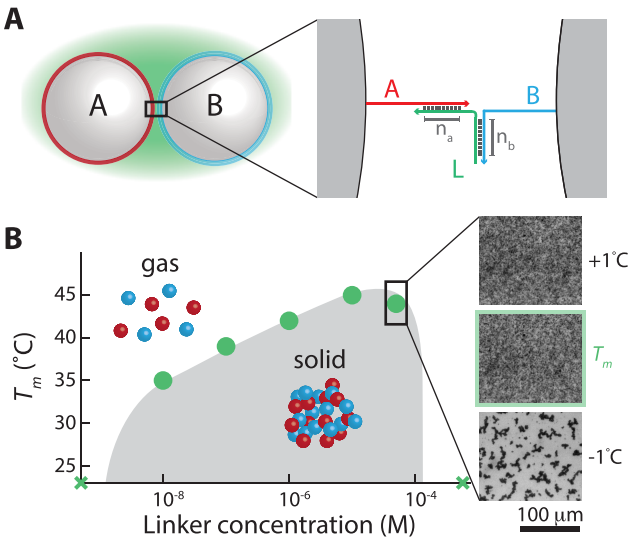

Figure 1. Overview of linker-mediated binding. (A) Our experimental system is composed of three single-stranded DNA sequences: grafted sequences A (red) and B (blue) tethered to colloidal particles and linker sequences L (green) dispersed in solution. Linkers are composed of two binding domains: one of n_a nucleotides complementary to A and another of n_b nucleotides complementary to B. (B) The temperature-linker concentration phase diagram shows a concentration-dependent solid−gas transition at low to intermediate linker concentrations and a re-entrant transition at high linker concentrations. We delineate the phase boundary by the melting temperature (T_m), defined as the temperature at which 50% of the particles are unbound. Green circles show measurements of melting temperatures, and green crosses represent samples that do not aggregate even at room temperature. The gray shaded region is a guide to the eye. Brightfield micrographs show the same suspension at temperatures above and below T_m. Both linker binding domains are 10 nt long for the data in (B).

RESULTS AND DISCUSSION

Colloidal Phase Behavior Using Symmetric Linkers. Linker-mediated interactions give rise to a gas−solid transition that can be tuned by changing the linker concentration and a re-entrant melting transition to the gas phase. Figure 1B shows an example of the generic temperature-linker concentration phase diagram for a symmetric linker with 10 nt-long binding domains. We measure the melting temperature of a colloidal

https://dx.doi.org/10.1021/acs.langmuir.9b03391
Langmuir XXXX, XXX, XXX−XXX

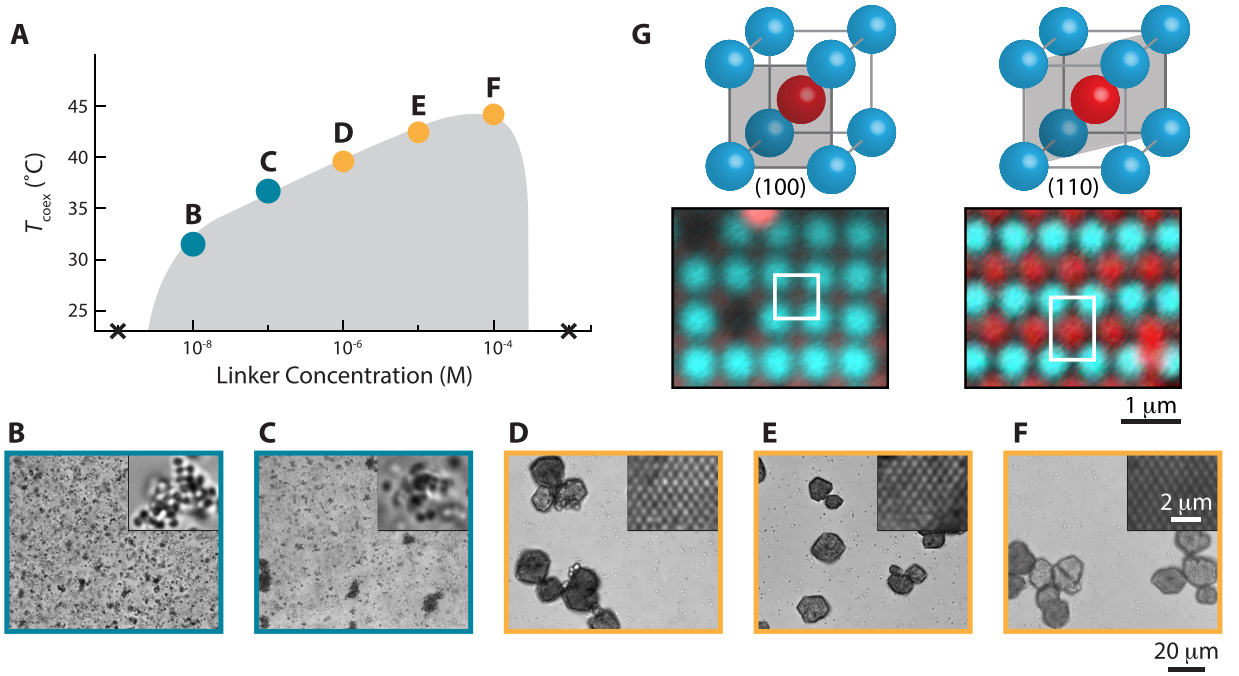

Figure 2. Linker-mediated crystallization. (A) The coexistence temperature as a function of linker concentration. Crosses represent conditions at which particles do not aggregate. Circles show experimental measurements of the temperatures at which crystals (orange) or disordered aggregates (blue) form. The gray shaded area is a guide to the eye. (B–F) Brightfield micrographs of the samples corresponding to the measurements in (A). (G) Confocal micrographs of the (100) plane (left) and (110) plane (right) of the crystals formed, along with illustrations of the CsCl structure.

gel for linker concentrations ranging from 1 nM to 100 μM. We find that particles do not aggregate below a linker concentration of roughly 10 nM. At linker concentrations between 10 nM and 100 μM, the melting temperature increases with increasing linker concentration. At linker concentrations greater than 100 μM, the particles cease to aggregate and exhibit a re-entrant transition to the gas phase. Reference 21 provides a detailed discussion of this phase behavior.

From the perspective of programmable self-assembly, the phase diagram illustrates two important aspects of linker-mediated binding: (1) the melting temperature can be tuned by changing the linker concentration; (2) there is a finite range of linker concentrations over which colloids assemble. Figure 1B shows that the melting transition between gas and gel can be tuned from roughly 35 to 45 °C by changing the linker concentration from 10 nM to 100 μM. This observation implies that linker-mediated interactions can be made stronger by increasing the linker concentration at a fixed temperature; however, this trend is bounded at high linker concentrations by the re-entrant transition to the gas phase. As we showed previously, this re-entrant transition is a generic feature of linker-mediated binding and results from the preferential coating of all grafted strands by the linkers, thus passivating the particles against assembly.[21] Therefore, there is necessarily a limited range of linker concentrations that can be used in practice, spanning roughly 5 orders of magnitude.

In principle, this ability to tune interactions by changing linker concentration could be used to match the binding affinities between DNA-coated colloids. However, this conclusion is inferred from the transition temperatures between a gas phase and a kinetically arrested gel phase. Whether or not linkers can direct the assembly of equilibrium structures, like crystals[9,12] or fully addressable, aperiodic packings of spheres,[13,14] remains untested. In fact, we note that there are currently no examples of micrometer-scale binary colloidal crystals assembled using symmetric linkers.

Crystallization. We explore the possibility that linkers can direct the assembly of equilibrium structures by attempting to form colloidal crystals along the gas–solid phase boundary. We use a linker with 9 nt-long binding domains for all crystallization experiments and dye the two particle species with different fluorescent dyes to determine the compositional order of the assembled structures. We perform crystallization experiments by first raising the sample to a temperature above melting, to create a homogeneous gas, and then lowering the temperature to just below melting. We target a temperature at which small clusters nucleate only after 30 min and call this temperature the "coexistence temperature" (T_{coex}). The coexistence temperature is typically within 0.5 °C of the measured melting temperature between gas and gel. However, because the two temperatures are determined by different methods and reflect coexistence between different phases, we give them different names. We finally incubate the sample overnight at the coexistence temperature and image the resulting structures that form using optical microscopy and confocal fluorescence microscopy.

We find that linkers can indeed direct the assembly of equilibrium structures over a range of linker concentrations. We perform crystallization experiments using linker concentrations ranging from 10 nM to 100 μM at order-of-magnitude increments (Figure 2A). At concentrations at or below 100 nM, the particles form small, disordered aggregates, which do not crystallize over time scales of roughly 24 h (Figure 2B,C). In contrast, at linker concentrations ranging from 1 μM to 100 μM, large, faceted crystals self-assemble (Figure 2D–F). Over the three-orders-of-magnitude range of linker concentration, the resulting crystals that form appear to have roughly the

https://dx.doi.org/10.1021/acs.langmuir.9b03391
Langmuir XXXX, XXX, XXX–XXX

same size, faceting, and abundance. We conclude that the crystals are isomorphic to cesium chloride (CsCl) on the basis of the confocal micrographs (Figure 2G) (see the Supporting Information for details about our identification of the crystalline order).

We hypothesize that crystals fail to form at the lowest concentrations due to kinetic limitations. Given that particle collisions are due entirely to Brownian motion and are thus random, particles must be able to rearrange locally, or "roll", along the surface of the assembling structure in order to crystallize.[12] Therefore, both binding and unbinding rates of DNA bridges must be fast relative to the rate of local particle motion to enable the rolling process.[30] Assuming the rate of binding is independent of temperature,[30] we estimate that the rate of unbinding of a DNA bridge decreases by a factor of roughly 50 from 45 °C, the highest melting temperature at which we observe crystallization, to 35 °C, the temperature at which we first observe kinetic arrest. Taking this argument a step further, we estimate that the magnitude of the unbinding rate of a DNA bridge decreases from 3 to 0.07 s^{-1} over the same range of temperatures. We estimate these rates by relating kinetic measurements of DNA hairpins of a known sequence[31] to our DNA sticky end sequences (see the Supporting Information). When the rates that we estimate are compared to the temperature-dependent rates of particle rolling that have been shown by Pine and co-workers to yield crystals,[12] k_{roll} = 0.4−0.1 s^{-1}, it is plausible that the relatively slow rate of unbinding at low linker concentrations could limit rolling and thus crystallization. Because Pine and co-workers do not report rolling rates for which crystallization is suppressed, additional measurements of rolling are required to confirm our hypothesis. Moreover, because crystallization is governed by a delicate balance of many other rates, which are in general also temperature dependent, we note that there may be other kinetic traps along the pathway to crystallization in addition to rolling.

Next, we explore the possibility that other crystal structures could be assembled from the same binary mixture by changing the linker sequences. The behavior of a generic binary system is prescribed by three pair interactions, which can be represented by an interaction matrix (Figure 3A). In the interaction matrix, each matrix element represents a single pair interaction between the particle species of the given row and the particle species of the given column. The interaction matrix is symmetric because the interactions between particles A and B are the same as the interactions between particles B and A. The three possible interactions are "like" interactions between A and A, "like" interactions between B and B, and "unlike" interactions between A and B. Each of these three interactions is prescribed by a separate linker sequence. Thus, the full interaction matrix of a system of particles is encoded by the combination of the sequences and concentrations of all linkers. As a result, we expect that the same set of particle species could be programmed to form different crystal structures by changing the linker mixture.

We test this idea in an experiment by creating three systems using the same binary mixture of DNA-coated colloids but different combinations of linkers. The first system we examine solely consists of "unlike" attractions between particles A and B. Here, the interactions are prescribed by a single linker sequence L_{AB} having one domain complementary to A and another domain complementary to B (Figure 3B). Next, we examine a system with solely "like" attractions between particles A. These interactions are prescribed again by a single linker sequence L_{AA}, in which both binding domains are complementary to particle A (Figure 3C). The third system we examine is one with "like" attractions between particles A and "unlike" attractions between particles A and B (Figure 3D). The interactions in this system are prescribed by a combination of the two linker species described above. All systems are crystallized as previously described and imaged using both brightfield and confocal microscopy.

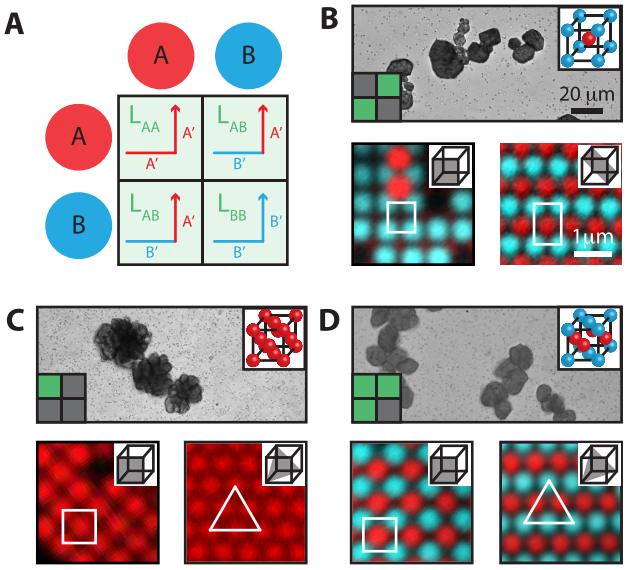

Figure 3. Assembling different crystal structures from the same colloidal building blocks. (A) The interaction matrix for a binary system of particles A and B has three pair interactions that are prescribed by three linker sequences: L_{AA}, L_{AB}, and L_{BB}. (B−D) (top) Brightfield micrographs showing assembled crystals, together with the corresponding interaction matrices and unit cells (insets). All brightfield images have the same scale, indicated in (B). (bottom) Confocal micrographs showing two different planes of the assembled crystals. Crystal planes are indicated in gray within the inset unit cell. We identify the assembled crystals to be CsCl (B), FCC (C), and CuAu (D). The linker concentrations for the three experiments are $[L_{AB}]$ = 10 μM (B); $[L_{AA}]$ = 10 μM (C); $[L_{AB}]$ = 50 μM, $[L_{AA}]$ = 5 μM (D). All confocal micrographs have the same scale, indicated in (B).

We find that each unique combination of interactions produces a unique crystal structure. In a solution of linkers L_{AB} that prescribe only "unlike" interactions, the crystals that form are isomorphic to CsCl (Figure 3B). In a solution of linkers L_{AA} that prescribe "like" interactions between particles A, we find that particles A form face centered cubic (FCC) crystals in a sea of unbound particles B (Figure 3C). Finally, when both L_{AB} and L_{AA} are mixed together, we observe a variety of outcomes that depend on the relative concentrations of the two linkers: At low concentrations of L_{AA} relative to L_{AB}, particles A and B form crystals that are isomorphic to CsCl, as before ($[L_{AA}]$ = 500 nM; $[L_{AB}]$ = 50 μM); at high concentrations of L_{AA} relative to L_{AB}, particles A form FCC crystals in a sea of particles B (Figure S5) ($[L_{AA}]$ = 5 μM; $[L_{AB}]$ = 5 μM); at intermediate concentrations, we find binary crystals that are isomorphic to copper gold (CuAu) (Figure 3D) ($[L_{AA}]$ = 5 μM; $[L_{AB}]$ = 50 μM). See Tables S3 and S4 for data confirming the various crystals structures that we observe.

https://dx.doi.org/10.1021/acs.langmuir.9b03391
Langmuir XXXX, XXX, XXX−XXX

The resulting crystal structures that we find are consistent with predictions[9,32] that assume all attractive interactions are short-range and exclusively prescribed by the linkers in solution. For systems with "unlike" attractions, corresponding to our single-linker case containing L_{AB}, computer simulations and free-energy calculations predict that CsCl-like crystals are thermodynamically stable.[32] For systems with "like" attractions, corresponding to L_{AA}, numerous theoretical predictions and experimental observations show that FCC should form in equilibrium.[12,33] Finally, for systems with strong "unlike" attraction and "weak" like attraction, corresponding to our mixed-linker case with a high concentration of L_{AB} and an intermediate concentration of L_{AA}, computer simulations predict that CuAu-like crystals are thermodynamically stable.[9] For each combination of linkers we explore, we observe the thermodynamically stable crystal phase, supporting our conclusion that linkers do in fact guide equilibrium assembly of DNA-coated colloids. Furthermore, these observations suggest that we should be able to use more complex mixtures of linkers to prescribe more complex interaction matrices.

One major advantage of linkers is the ability to fine-tune the interactions via the linker concentrations in solution. It is through this approach that we are able to observe a range of possible outcomes in our mixed-linker experiments combining L_{AB} and L_{AA}. In other words, linker-mediated interactions are not simply "on" or "off". Instead, their strengths can be tuned continuously. The combination of these two design parameters, linker sequence and linker concentration, adds considerable versatility to linker-mediated self-assembly of DNA-coated colloids.

Colloidal Phase Behavior Using Asymmetric Linkers. Whereas our experiments so far have focused on symmetric linkers, previous reports have focused primarily on a variant: asymmetric linkers. Asymmetric linkers, because they bind more strongly to one grafted sequence than the other, could have a variety of unique functions compared to symmetric linkers. Indeed, there are a number of interesting examples in the literature, including coating particles with DNA "sticky ends",[7,16] making polygamous particles,[18] tuning the flexibility and length of the DNA coating,[12,26] and making patterned DNA-functionalized surfaces.[24] In this section, we explore how linker-mediated interactions between colloids and the corresponding phase behavior change as we transition from symmetric to asymmetric linkers.

To characterize the role of asymmetry, we measure the melting temperature of a colloidal gel assembled by linkers with increasing asymmetry. We increase asymmetry by changing the number of nucleotides in the A binding domain from 7 to 15 nt, keeping the length of the B binding domain fixed at 8, 9, or 10 nt. We then measure the melting temperature as a function of increasing linker concentration, as we did previously for symmetric linkers (Figure 1B). We quantify the shape of the phase boundaries by measuring two quantities: T_m^* and ΔT_m (Figure 4A). T_m^* is the melting temperature at 50 μM linker concentration; ΔT_m is the change in melting temperature over the roughly "linear portion", between linker concentrations of 100 nM−10 μM, of the T_m versus $\log(C_l^0)$ phase boundary. Because crystallization experiments require an overnight incubation, we focus solely on quantifying the melting transition between gel and gas in order to explore a wide range of linker architectures. Therefore, we cannot conclude from these experiments alone whether or not asymmetric linkers can also lead to crystallization. However, as

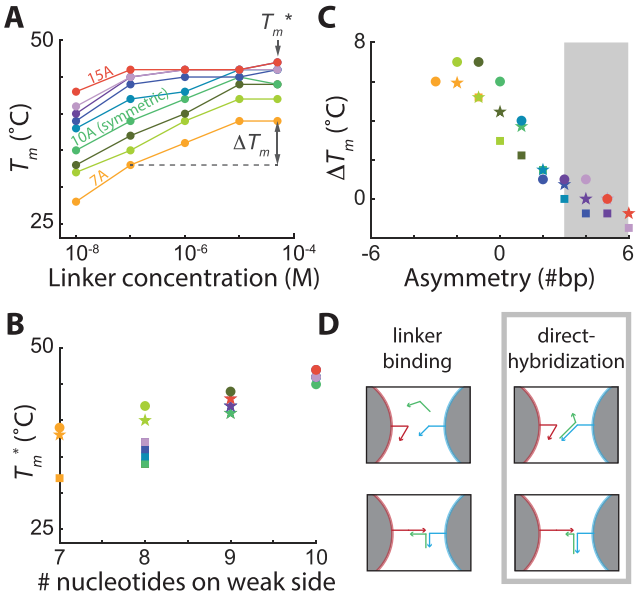

Figure 4. Effects of linker asymmetry on the phase behavior. (A) Experimental measurements of the melting temperature for a 21 nt symmetric linker (light green) upon increasing (blue to red) and decreasing (green to orange) the length of the A binding domain. Points correspond to data; lines are guides for the eye. (B) The melting temperature at a linker concentration of 50 μM (T_m^*) as a function of the number of base pairs in the shortest binding domain. Symbols correspond to linkers with B binding domains of length 8 nt (squares), 9 nt (stars), and 10 nt (circles). Colors correspond to the length of the A binding domain using the same color scheme as shown in (A). (C) The difference in melting temperatures at linker concentrations of 100 nM and 50 μM, referred to as ΔT_m, versus the difference in length of the two linker binding domains. A difference in length of 0 bp corresponds to the symmetric case. (D) We hypothesize that symmetric linkers form bridges by the three-strand reaction $A + L + B$. The highly asymmetric case resembles direct hybridization in which bridges are formed by the reaction between two DNA species bound to particles' surfaces: a grafted strand and a half-bridge in this case. The gray boxed figure corresponds to the gray shaded region of (C).

shown previously, the melting temperature and coexistence temperature are roughly equal to one another, so we expect the equilibrium phase boundary to shift in a similar fashion.

The increase of the linker asymmetry has pronounced effects on the nature of the phase boundary between gas and gel. We focus first on the isolated case of a linker with 10 nt in the B binding domain and 7−15 nt in the A binding domain (Figure 4A). We find colloidal gels at room temperature over the same range of linker concentrations, regardless of asymmetry. When the A binding domain is lengthened, three dominant trends are produced: (1) The melting temperature increases at all linker concentrations. (2) The melting temperature becomes a weaker function of the linker concentration, resulting in a phase boundary that appears to progressively "flatten". (3) The previous two effects tend to "saturate" for very asymmetric linkers. When the binding domain is shortened instead of lengthened, it appears to have a subtler effect. The melting temperature decreases at all linker concentrations, but the phase boundary does not flatten appreciably at higher linker concentrations.

The shorter of the two binding domains largely determines the melting temperature of the assembled colloidal gels. Figure

https://dx.doi.org/10.1021/acs.langmuir.9b03391
Langmuir XXXX, XXX, XXX−XXX

4B shows measurements of T_m^* as a function of the number of bases in the shorter binding domain for many asymmetric linkers. We find a roughly linear relationship between the number of nucleotides in the shorter binding domain and T_m^*. There is also a small dependence of T_m^* on the number of bases in the longer binding domain. Specifically, we observe a slight increase in T_m^* upon increasing the length of the longer binding domain, which becomes more prominent when the shorter binding domain is small. These results indicate that the melting temperature is most strongly influenced by the affinity of the weaker of the two binding domains.

We can understand these observations by considering the routes by which particles are linked together by DNA bridges. We clearly observe a dependence of T_m^* on the length of the shortest binding domain. We understand this dependence by considering the limiting case in which the linker is highly asymmetric and is therefore always bound on its strong side. In this limit, the only way for bridges to break is for the short domain to rupture. Thus, the melting temperature would be determined by the affinity of the short domain, as observed. However, we also see some secondary trends within the data. Specifically, T_m^* slightly increases with an increasing length of the long binding domain. This secondary trend arises from the fact that not all experiments have reached the highly asymmetric limit. In fact, many linkers have asymmetries of only 0, 1, or 2 nt. In these cases, the affinities of both the long and short binding domains contribute to the melting temperature. Lastly, because small asymmetries in the number of nucleotides lead to large differences in the affinities of the two domains when the weak side is short, this effect becomes more significant for the shortest binding domains, again as observed.

We find that the difference in lengths between the two binding domains also has a strong effect on the slope of the melting temperature with respect to the linker concentration. We divide our asymmetric linkers into two categories: Linkers with positive asymmetry have a longer A binding domain, and linkers with negative asymmetry have a longer B binding domain. We find that ΔT_m decreases with increasing asymmetry (Figure 4C). Above an asymmetry of roughly 3 nt, we find that the change in melting temperature ΔT_m approaches 0, effectively decoupling T_m from the linker concentration (Figure 4C, gray shaded region). Interestingly, the trends do not appear to be symmetric about an asymmetry of 0 nt and instead appear to be centered about an asymmetry of −2 nt. Unfortunately, we were unable to explore a comparable range of negative asymmetries since the particles do not aggregate for such short linkers.

Our measurements of ΔT_m are consistent with our hypotheses from above and show that linker-based systems can have different limiting behaviors: Their behavior can be sensitive to the concentration of free linkers dispersed in solution, or they can behave like DNA-coated colloids interacting by direct binding. Interactions due to symmetric linkers require that both halves of the linker bind in order to form a bridge, which they do with equal probability (Figure 4D). Since this probability depends on the linker concentration, the resultant interactions also depend on the linker concentration. However, when one side of the linker becomes much stronger than the other, linkers will preferentially coat the strong-binding species. This effectively functionalizes the strong-binding particle species with sticky ends of the weak binding domain, leading to interactions that resemble direct binding (Figure 4D). Returning to our observation that ΔT_m is not symmetric about an asymmetry of 0 nt, we hypothesize that this result is due to the fact that the binding affinities of the two sides of most linkers, even symmetric ones, will in general be different owing to differences in their sequences. Indeed, a quick comparison of the free energies of the two binding domains shows that even symmetric linkers can have binding affinities that vary by 0−2 kcal/mol (see Table S2). Thus, rather than being controlled by asymmetry in the number of base pairs formed, we hypothesize that ΔT_m is instead determined by the relative affinities of the two binding domains.

We confirm our molecular-scale description of the asymmetric phase behavior using a mean-field model. Specifically, we predict the melting temperature and the number of the molecular species in the gap between particles using a validated model of linker-mediated binding.[21,34] In contrast to earlier models that were developed to describe direct binding between DNA-coated colloids,[16,17,35] our model of linker-mediated binding can predict both the number of bridges linking particles together and the number of other molecular species that occur in equilibrium. The specific molecular species that we are interested in are the "half-bridges" of a linker bound to a single grafted strand A or B. We calculate the number of half-bridges at the melting transition for two asymmetric linkers: one in which the A binding domain is longer and another in which the B binding domain is longer (Figure 5).

Both asymmetric linkers exhibit a plateau in the melting temperature above linker concentrations of roughly 100 nM,

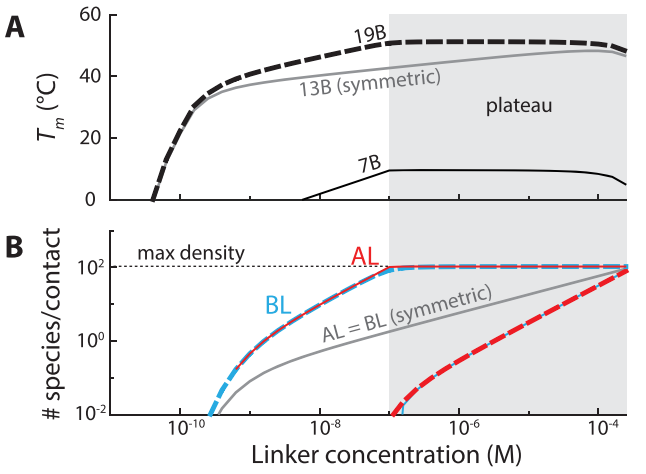

Figure 5. Model predictions of asymmetric-linker phase behavior. (A) The melting temperature as a function of linker concentration for three linker species with 13 nt in the A binding domain: a symmetric linker (gray solid line), an asymmetric linker with 19 nt in the B domain (black solid line), and an asymmetric linker with 7 nt in the B domain (black dashed line). Both asymmetric linkers exhibit a plateau in the melting temperature at high linker concentrations (gray shaded region). Predictions are made using the model described in ref 21. (B) Model predictions of the number of half-bridges AL (red) and BL (blue) in the gap between two interacting particles as a function of linker concentration. Dashed lines correspond to the 19 nt asymmetric linker, and solid lines correspond to the 7 nt asymmetric linker. The strong binding domain causes the linkers to fully coat the surface of one particle within the plateau region. The maximum density of bound complexes is shown by the horizontal dashed line.

https://dx.doi.org/10.1021/acs.langmuir.9b03391
Langmuir XXXX, XXX, XXX−XXX

consistent with our experimental observations (Figure 5A, gray shaded region). Moreover, we find that the stronger linker binding domain exhibits a plateau in the number of half-bridges (AL or BL) at linker concentrations above 100 nM (Figure 5B, gray shaded region). When the B domain is stronger, half-bridges between linker and particle B saturate the total number of available binding sites. At these elevated melting temperatures, the shorter A binding domain is unable to bind, leaving particle A relatively bare and free to form full-bridges with the linker-functionalized B particles. The results are similar for the other linker but with the roles of the A and B particles reversed. In both cases, the model predictions reproduce the same qualitative trends we observe in our experiments and show that particles become coated with linkers, resulting in interactions analogous to the binding between particles coated in complementary sequences.

Finally, we test the possibility that asymmetric linkers might help to circumvent the kinetic limitations we encountered for symmetric linkers. Since increasing the linker asymmetry increases the melting temperature at a fixed linker concentration and thus the off rate of DNA hybridization, we hypothesize that asymmetric linkers might have faster rolling dynamics than symmetric linkers. To test this hypothesis, we perform two crystallization experiments at the same linker concentration: one using a symmetric linker with 9 nt binding domains and another using an asymmetric linker with one 9 nt binding domain and one 14 nt binding domain. Interestingly, we find that the asymmetric linker produces crystals after roughly 24 h at 100 nM linker concentration. As before, the symmetric linker yields only amorphous aggregates at the same concentration (see the Supporting Information and Figure S4). Because increasing the linker asymmetry increases the melting temperature by roughly 10 °C, it is plausible that the crystallization that we observe for asymmetric linkers comes from an increase in the off rate of the weak binding domain. Future studies will explore this possibility further.

In summary, asymmetry in the linker architecture leads to unique phase behavior and might help to overcome kinetic bottlenecks. Interactions that are largely independent of linker concentration can be a design advantage or disadvantage, depending on the goals of the design. When one side of the linker is made to be significantly longer than the other, it is possible to coat colloidal particles with weak binding "sticky ends". This strategy provides another route to separating the binding instructions from the colloidal particles themselves. For example, the sequence and surface density of sticky ends can be adjusted without resynthesizing the particles by swapping out or mixing different asymmetric linkers. Asymmetric linkers could also be useful for systems that require spatial patterning of specific DNA sequences or need to be robust to variations in the solution conditions. However, we highlight one significant drawback of asymmetric linkers: the linkers do not bind and unbind dynamically. Therefore, encoding a large number of pair interactions for a single particle species requires one to mix many asymmetric linkers, which bind irreversibly, effectively diluting the surface density of any one sticky end sequence on the particles' surfaces. Moreover, using asymmetric linkers to specify an interaction matrix of P particles would require one to design a unique "sticky end" sequence for each pair interaction, up to a maximum of $P(P + 1)/2$ sequences. Thus, it will be hard to specify the dozens of specific interactions required for fully addressable assembly in this way. In contrast, the specification of the same number of interactions using symmetric linkers requires only P unique sequences. These P sequences specify the particle identifications. The linker sequences are then constructed by joining together pairs of sequence domains that are complementary to the two particle identifications.

SUMMARY AND CONCLUSIONS

We have shown that encoding colloidal interactions in linker sequences is a powerful design framework for complex self-assembly of DNA-coated colloids. First, we showed that linkers can direct colloids to self-assemble into crystals over a wide range of linker concentrations. The structures of the crystals that formed matched predictions based solely on the attractive interactions prescribed by the linkers in solution. This result demonstrates that linker-mediated assembly is a viable method for programming complex equilibrium architectures. Second, we showed that the same building blocks can be directed to form different crystal lattices by mixing and matching linker sequences. This result highlights the versatility of linker-encoded interactions: The instructions specifying assembly can be separated from the building blocks themselves. These results extend our previous findings to show that not only can linkers prescribe and tune many interactions but also these interactions can direct the assembly of equilibrium structures.

We have also explored linkers designed to be symmetric, highly asymmetric, or somewhere in between. On one hand, highly asymmetric linkers remove the tunability of the binding strength with respect to linker concentration, which could limit their utility for fully addressable assembly. On the other hand, asymmetric linkers can be used as a versatile method to prepare particles with adjustable "sticky end" sequences and densities without resynthesizing the colloids. Furthermore, asymmetric linkers might also be able to overcome kinetic bottlenecks to crystallization at the lowest linker concentrations. Although we have not explored this possibility here, we highlight that symmetric and asymmetric linkers could be combined together in the same experiment to produce new outcomes. Thus, the choice of the most appropriate linker depends on the application.

While this work focuses on the equilibrium self-assembly of relatively simple colloidal crystals at fixed temperatures, linkers could also be used in a variety of other contexts. For example, the combination of many linkers with different binding affinities could aid in hierarchical assembly, in which a target design is assembled in a series of discrete steps. Furthermore, linkers could be used in conjunction with a variety of other building blocks, not just uniformly coated colloidal spheres. Addressable structures could be self-assembled in bulk from fewer particle species[15] by combining the valence-limited interactions of patchy particles[36,37] with the sequence-design benefits of linkers. Alternatively, particles with mobile tethers like DNA-coated emulsion droplets[38−40] could also have emergent valence-limited interactions that influence their assembly. Finally, the applications of linker-mediated design need not be limited to self-assembly. The aggregation of specific particle species in response to the presence of specific linker sequences in solution could open new possibilities for purification or detection of DNA sequences,[41] which could have diagnostic applications.

https://dx.doi.org/10.1021/acs.langmuir.9b03391
Langmuir XXXX, XXX, XXX−XXX

■ ASSOCIATED CONTENT

Supporting Information

The Supporting Information is available free of charge at https://pubs.acs.org/doi/10.1021/acs.langmuir.9b03391.

Detailed experimental methods, DNA sequences, and DNA thermodynamics (PDF)

■ AUTHOR INFORMATION

Corresponding Author

W. Benjamin Rogers − *Martin A. Fisher School of Physics, Brandeis University, Waltham, Massachusetts 02453, United States*; orcid.org/0000-0001-8587-8215; Email: wrogers@brandeis.edu

Authors

Janna Lowensohn − *Martin A. Fisher School of Physics, Brandeis University, Waltham, Massachusetts 02453, United States*

Alexander Hensley − *Martin A. Fisher School of Physics, Brandeis University, Waltham, Massachusetts 02453, United States*

Michael Perlow-Zelman − *Martin A. Fisher School of Physics, Brandeis University, Waltham, Massachusetts 02453, United States*

Complete contact information is available at: https://pubs.acs.org/10.1021/acs.langmuir.9b03391

Notes

The authors declare no competing financial interest.

■ ACKNOWLEDGMENTS

The authors thank Bortolo Matteo Mognetti, Eric Weeks, Matthew Peterson, and Aparna Baskaran for helpful discussions. We also thank the National Science Foundation for financial support (DMR-1710112).

■ REFERENCES

(1) Mirkin, C. A.; Letsinger, R. L.; Mucic, R. C.; Storhoff, J. J. A DNA-Based Method for Rationally Assembling Nanoparticles into Macroscopic Materials. *Nature* **1996**, *382*, 607.

(2) Alivisatos, A. P.; Johnsson, K. P.; Peng, X.; Wilson, T. E.; Loweth, C. J.; Bruchez, M. P., Jr; Schultz, P. G. Organization of 'Nanocrystal Molecules' Using DNA. *Nature* **1996**, *382*, 609.

(3) SantaLucia, J., Jr; Hicks, D. The Thermodynamics of DNA Structural Motifs. *Annu. Rev. Biophys. Biomol. Struct.* **2004**, *33*, 415−440.

(4) Jones, M. R.; Seeman, N. C.; Mirkin, C. A. Programmable Materials and the Nature of the DNA Bond. *Science* **2015**, *347*, 1260901.

(5) Rogers, W. B.; Shih, W. M.; Manoharan, V. N. Using DNA to Program the Self-Assembly of Colloidal Nanoparticles and Microparticles. *Nat. Rev. Mater.* **2016**, *1*, 16008.

(6) Biancaniello, P. L.; Kim, A. J.; Crocker, J. C. Colloidal Interactions and Self-Assembly Using DNA Hybridization. *Phys. Rev. Lett.* **2005**, *94*, 058302.

(7) Park, S. Y.; Lytton-Jean, A. K.; Lee, B.; Weigand, S.; Schatz, G. C.; Mirkin, C. A. DNA-Programmable Nanoparticle Crystallization. *Nature* **2008**, *451*, 553.

(8) Nykypanchuk, D.; Maye, M. M.; Van Der Lelie, D.; Gang, O. DNA-Guided Crystallization of Colloidal Nanoparticles. *Nature* **2008**, *451*, 549.

(9) Casey, M. T.; Scarlett, R. T.; Rogers, W. B.; Jenkins, I.; Sinno, T.; Crocker, J. C. Driving Diffusionless Transformations in Colloidal Crystals Using DNA Handshaking. *Nat. Commun.* **2012**, *3*, 1209.

(10) Macfarlane, R. J.; Lee, B.; Jones, M. R.; Harris, N.; Schatz, G. C.; Mirkin, C. A. Nanoparticle Superlattice Engineering with DNA. *Science* **2011**, *334*, 204−208.

(11) Rogers, W. B.; Manoharan, V. N. Programming Colloidal Phase Transitions with DNA Strand Displacement. *Science* **2015**, *347*, 639−642.

(12) Wang, Y.; Wang, Y.; Zheng, X.; Ducrot, É.; Yodh, J. S.; Weck, M.; Pine, D. J. Crystallization of DNA-Coated Colloids. *Nat. Commun.* **2015**, *6*, 7253.

(13) Hormoz, S.; Brenner, M. P. Design Principles for Self-Assembly with Short-Range Interactions. *Proc. Natl. Acad. Sci. U. S. A.* **2011**, *108*, 5193−5198.

(14) Zeravcic, Z.; Manoharan, V. N.; Brenner, M. P. Size Limits of Self-Assembled Colloidal Structures Made Using Specific Interactions. *Proc. Natl. Acad. Sci. U. S. A.* **2014**, *111*, 15918−15923.

(15) Halverson, J. D.; Tkachenko, A. V. DNA-Programmed Mesoscopic Architecture. *Phys. Rev. E* **2013**, *87*, 062310.

(16) Dreyfus, R.; Leunissen, M. E.; Sha, R.; Tkachenko, A. V.; Seeman, N. C.; Pine, D. J.; Chaikin, P. M. Simple Quantitative Model for the Reversible Association of DNA Coated Colloids. *Phys. Rev. Lett.* **2009**, *102*, 048301.

(17) Rogers, W. B.; Crocker, J. C. Direct Measurements of DNA-Mediated Colloidal Interactions and Their Quantitative Modeling. *Proc. Natl. Acad. Sci. U. S. A.* **2011**, *108*, 15687−15692.

(18) Wu, K.-T.; Feng, L.; Sha, R.; Dreyfus, R.; Grosberg, A. Y.; Seeman, N. C.; Chaikin, P. M. Polygamous Particles. *Proc. Natl. Acad. Sci. U. S. A.* **2012**, *109*, 18731−18736.

(19) Xiong, H.; van der Lelie, D.; Gang, O. DNA Linker-Mediated Crystallization of Nanocolloids. *J. Am. Chem. Soc.* **2008**, *130*, 2442−2443.

(20) Xiong, H.; van der Lelie, D.; Gang, O. Phase Behavior of Nanoparticles Assembled by DNA Linkers. *Phys. Rev. Lett.* **2009**, *102*, 015504.

(21) Lowensohn, J.; Oyarzún, B.; Narváez Paliza, G.; Mognetti, B. M.; Rogers, W. B. Linker-Mediated Phase Behavior of DNA-Coated Colloids. *Phys. Rev. X* **2019**, *9*, 041054.

(22) Wu, K.-T.; Feng, L.; Sha, R.; Dreyfus, R.; Grosberg, A. Y.; Seeman, N. C.; Chaikin, P. M. Kinetics of DNA-Coated Sticky Particles. *Phys. Rev. E* **2013**, *88*, 022304.

(23) Wang, M. X.; Brodin, J. D.; Millan, J. A.; Seo, S. E.; Girard, M.; Olvera de la Cruz, M.; Lee, B.; Mirkin, C. A. Altering DNA-Programmable Colloidal Crystallization Paths by Modulating Particle Repulsion. *Nano Lett.* **2017**, *17*, 5126−5132.

(24) Myers, B. D.; Lin, Q.-Y.; Wu, H.; Luijten, E.; Mirkin, C. A.; Dravid, V. P. Size-Selective Nanoparticle Assembly on Substrates by DNA Density Patterning. *ACS Nano* **2016**, *10*, 5679−5686.

(25) Thaner, R. V.; Eryazici, I.; Macfarlane, R. J.; Brown, K. A.; Lee, B.; Nguyen, S. T.; Mirkin, C. A. The Significance of Multivalent Bonding Motifs and "Bond Order" in DNA-Directed Nanoparticle Crystallization. *J. Am. Chem. Soc.* **2016**, *138*, 6119−6122.

(26) Thaner, R. V.; Kim, Y.; Li, T. I.; Macfarlane, R. J.; Nguyen, S. T.; Olvera de la Cruz, M.; Mirkin, C. A. Entropy-Driven Crystallization Behavior in DNA-Mediated Nanoparticle Assembly. *Nano Lett.* **2015**, *15*, 5545−5551.

(27) Lin, Q.-Y.; Li, Z.; Brown, K. A.; O'Brien, M. N.; Ross, M. B.; Zhou, Y.; Butun, S.; Chen, P.-C.; Schatz, G. C.; Dravid, V. P.; Aydin, K.; Mirkin, C. A. Strong Coupling Between Plasmonic Gap Modes and Photonic Lattice Modes in DNA-Assembled Gold Nanocube Arrays. *Nano Lett.* **2015**, *15*, 4699−4703.

(28) Oh, J. S.; Wang, Y.; Pine, D. J.; Yi, G.-R. High-Density PEO-b-DNA Brushes on Polymer Particles for Colloidal Superstructures. *Chem. Mater.* **2015**, *27*, 8337−8344.

(29) Kim, A. J.; Manoharan, V. N.; Crocker, J. C. Swelling-Based Method for Preparing Stable, Functionalized Polymer Colloids. *J. Am. Chem. Soc.* **2005**, *127*, 1592−1593.

(30) Rogers, W. B.; Sinno, T.; Crocker, J. C. Kinetics and Non-exponential Binding of DNA-Coated Colloids. *Soft Matter* **2013**, *9*, 6412−6417.

(31) Bonnet, G.; Krichevsky, O.; Libchaber, A. Kinetics of Conformational Fluctuations in DNA Hairpin-Loops. *Proc. Natl. Acad. Sci. U. S. A.* **1998**, *95*, 8602−8606.
(32) Scarlett, R. T.; Ung, M. T.; Crocker, J. C.; Sinno, T. A Mechanistic View of Binary Colloidal Superlattice Formation Using DNA-Directed Interactions. *Soft Matter* **2011**, *7*, 1912−1925.
(33) Binder, K.; Virnau, P.; Statt, A. Perspective: The Asakura Oosawa Model: A Colloid Prototype for Bulk and Interfacial Phase Behavior. *J. Chem. Phys.* **2014**, *141*, 140901.
(34) Di Michele, L.; Bachmann, S. J.; Parolini, L.; Mognetti, B. M. Communication: Free Energy of Ligand-Receptor Systems Forming Multimeric Complexes. *J. Chem. Phys.* **2016**, *144*, 161104.
(35) Varilly, P.; Angioletti-Uberti, S.; Mognetti, B. M.; Frenkel, D. A General Theory of DNA-Mediated and Other Valence-Limited Colloidal Interactions. *J. Chem. Phys.* **2012**, *137*, 094108.
(36) Wang, Y.; Wang, Y.; Breed, D. R.; Manoharan, V. N.; Feng, L.; Hollingsworth, A. D.; Weck, M.; Pine, D. J. Colloids with Valence and Specific Directional Bonding. *Nature* **2012**, *491*, 51.
(37) Ben Zion, M. Y.; He, X.; Maass, C. C.; Sha, R.; Seeman, N. C.; Chaikin, P. M. Self-Assembled Three-Dimensional Chiral Colloidal Architecture. *Science* **2017**, *358*, 633−636.
(38) Joshi, D.; Bargteil, D.; Caciagli, A.; Burelbach, J.; Xing, Z.; Nunes, A. S.; Pinto, D. E.; Araújo, N. A.; Brujic, J.; Eiser, E. Kinetic Control of the Coverage of Oil Droplets by DNA-Functionalized Colloids. *Sci. Adv.* **2016**, *2*, No. e1600881.
(39) Feng, L.; Pontani, L.-L.; Dreyfus, R.; Chaikin, P.; Brujic, J. Specificity, Flexibility and Valence of DNA Bonds Guide Emulsion Architecture. *Soft Matter* **2013**, *9*, 9816−9823.
(40) McMullen, A.; Holmes-Cerfon, M.; Sciortino, F.; Grosberg, A. Y.; Brujic, J. Freely Jointed Polymers Made of Droplets. *Phys. Rev. Lett.* **2018**, *121*, 138002.
(41) Reynolds, R. A.; Mirkin, C. A.; Letsinger, R. L. Homogeneous, Nanoparticle-Based Quantitative Colorimetric Detection of Oligonucleotides. *J. Am. Chem. Soc.* **2000**, *122*, 3795−3796.

https://dx.doi.org/10.1021/acs.langmuir.9b03391
Langmuir XXXX, XXX, XXX−XXX